The Origin and Development of Transient Coronal Holes

S. W. Kahler

Air Force Research Laboratory, Space Vehicles Directorate

H. S. Hudson

Solar Physics Research Corporation

Short title: THE ORIGIN AND DEVELOPMENT OF TRANSIENT CORONAL HOLES

Abstract. Solar transient coronal holes (TCHs) are short-lived ($\leq$ 2 days) regions of dimmed X-ray intensity sometimes observed in association with coronal mass ejections. These features, first discovered from Skylab observations, can occur in magnetic unipolar regions on either side of the X-ray posteruptive arcades. They have been suggested as the magnetically open footpoints of associated transient flux ropes observed at 1 AU. We have used images from the Yohkoh Soft X-ray Telescope (SXT) to study the development of 19 TCH events obtained in a survey of 9 years of Yohkoh observations. We find that the boundaries of the TCHs are never static. The boundaries closer to the magnetic neutral line generally move away from it as the closed-loop X-ray arcades expand. In addition, previously closed coronal loops at the ends of the arcades often continue to expand and open on the outer boundaries of the TCHs. These processes typically last for hours. The arcade brightenings do not extend into the full areas of the TCHs. The TCHs tend to disappear only by a net contraction of the boundaries, rather than by brightening within their boundaries. The location of a TCH appears to coincide with a large scale curvature of the magnetic neutral line or the occurrence of a nearby active region at one end of the coronal eruption. This distinguishes the formation of TCHs from the arcade development, suggesting that there is no requirement for a pair of TCHs or even any TCH to be formed in an eruptive event. The moving magnetic boundaries, uniformly dark interiors, and short lifetimes of TCHs pose significant problems for the interpretation that TCHs are footpoints of interplanetary magnetic flux ropes.

1. Introduction

The term transient coronal hole (TCH) was introduced by Rust (1983) to describe voids in Skylab X-ray images that occurred within 0.2 Ro of Hα filament eruptions associated with long-decay X-ray enhancements (LDEs). In 11 of 21 candidate events Rust found voids that "were as dark as nearby 'permanent' coronal holes." The search for TCHs was motivated by the idea that transient high speed wind flows following coronal mass ejections (CMEs) could come from the same kind of open magnetic structure that gives rise to long-lived high speed wind streams at 1 AU. The short (< 48 hrs) lifetimes of the Skylab TCHs further suggested (Rust, 1983) an association with interplanetary magnetic clouds.

Following the Skylab mission, the next opportunity to observe TCHs in solar soft X-ray images occurred when the Yohkoh Soft X-ray Telescope (SXT) began observations in 1991 (Tsuneta et al., 1991). TCHs in SXT data and their associations with CMEs were reported by Watanabe et al.(1992), Watari et al.(1995), Manoharan et al. (1996), Hudson and Webb (1997), and Khan et al. (1998). TCHs have also been observed (Thompson et al., 1998) in data from the Extreme ultraviolet Imaging Telescope (EIT) on the SOHO spacecraft. TCHs are only one of at least four classes of X-ray dimming signatures seen in association with CMEs (Hudson and Webb, 1997). The defining characteristics of X-ray TCHs (Hudson and Webb, 1997) are proximity to an arcade development and a transient (≤ 1 day) decrease in brightness approaching that of the long-lived coronal holes. They often form in association with S-shaped (sigmoid) active-region structures (Sterling et al., 2000), and as with long-lived holes, they lie in magnetically unipolar regions. Several kinds of dimmings showing coronal mass loss associated with CMEs have been detected by image subtraction (Sterling and Hudson, 1997; Hudson et al., 1998; Thompson et al., 2000). However, as Sterling and Hudson (1997) point out, often it may not be appropriate to equate such dimming regions with TCHs. We will adhere to a stricter TCH definition that the TCH be easily observed in direct SXT images, rather than in a difference image.

Only a limited number of TCHs have been discussed in the references cited above, but the basic interpretation of Rust (1983), that TCHs are solar source regions of CMEs observed in interplanetary space, has been adapted to recent observations of magnetic structures at 1 AU. Twin dimmings have been suggested (Sterling and Hudson, 1997; Webb et al., 2000a) as the source of the footpoints of a magnetic flux rope. Webb et al. (2000b) interpreted double dimming regions seen in the EIT observations of an arcade on May 12, 1997 as the footpoints of a magnetic cloud observed at 1 AU on May 15, 1997. They found that the orientation, handedness, and magnetic flux of the dimming regions matched well with those of the associated interplanetary magnetic flux rope. Smith et al. (1997) and Larson et al. (1997) also interpreted a coronal dimming region observed between several active regions on October 14, 1995 as one footpoint of a flux rope observed at 1 AU on October 18-20. The dimming regions of these two specific cases meet our criteria for TCHs.

If the flux ropes detected as magnetic clouds at 1 AU do have their footpoints in TCHs, then the shapes and sizes of the TCHs should reflect the solar magnetic connectivity between the imbedded coronal fields and the flux rope fields at 1 AU. Larson et al. (1997) used solar electrons to deduce that interior sections of the negative polarity leg of the October 18-20, 1995 flux rope were magnetically disconnected from the identified TCH source region. They suggested that parts of the flux-rope leg had become disconnected by reconnection with adjacent field lines. In a survey of 48 magnetic clouds Shodhan et al. (2000) used counterstreaming electron heat fluxes to determine the connectivity of the magnetic clouds to their solar footpoints. Some clouds were completely disconnected from one footpoint, others were completely connected to both footpoints, and the periods of complete connection were randomly distributed throughout the clouds. If we assume that the footpoints of the clouds are TCHs, then the disconnection regions of the clouds might correspond to the regions of the TCH which have also closed in the corona.

Even without assuming a close correspondence between TCH areas and connected regions of magnetic clouds, the manner in which the TCH boundaries change could be indicative of the reconnection process. In two extreme hypothetical cases, TCHs could simply shrink inward from their boundaries with no interior brightenings, indicating no magnetic reconnections of internal field lines, or they could begin to brighten internally, indicating reconnection occurring along the internal field lines. Rust (1983) showed that the former process occurred in one of the Skylab TCHs, but a systematic study has not been done to determine the general process by which TCHs disappear, and by inference, re-establish closed magnetic fields.

A second reason for a study of TCH disappearances is that the process in which magnetic reconnection occurs at long-lived CH boundaries is still undefined. It is presumed that reconnection must occur at long-lived CH boundaries, particularly at the long-lived co-rotating holes (Wang and Sheeley, 1993; Wang et al., 1996), where differential rotation acts to distort the CH boundaries. A limited study of the time and size scales of CH reconnection was carried out with Skylab X-ray data by Kahler and Moses (1990), but no similar work has been done with the SXT data. An examination of the processes occurring at TCH boundaries could provide insights into the processes at work in CH boundaries as well. For these reasons we carry out a survey of changes in TCH boundaries using the SXT data.

2. Data Analysis

2.1. Data selection

The TCHs used in the study were selected in several ways. We used an SXT video movie of full disk frames to examine candidate TCH events that were reported in the literature, included in a list of associated halo CME events (D.F. Webb, private comm.), followed by magnetic clouds identified in magnetic field data from the WIND spacecraft, or found in a cursory examination of the SXT video for 1999 and 2000. In each case the TCH was sought following an eruptive X-ray event, and a distinct region of newly dimmed X-ray intensity was required for selection. Cases in which the TCH was only marginally observable or significant data gaps precluded good coverage of the TCH development were eliminated. This selection process favored TCHs outside active regions and near disk center and those in which the SXT flare observation mode was not initiated. The exclusion of LDE flares because of the Yohkoh flare mode results in a large decrease of candidate events in comparison with the Skylab observations (Rust 1983). A total of 19 events were selected from the SXT data and are listed in Table 1. For each event we give the date and time of first SXT image showing the TCH, the approximate TCH disk location near the time of formation, and other information discussed in detail in Section 2.2. When a pair of TCHs was observed, the data in the table refer to the larger of the pair.

Each TCH was examined by making a movie of image sequences using only the long exposures in a single filter. The thin Al filter was used for TCHs in 1991 and 1992, and after the loss of the SXT prefilter late in 1992, only the thicker AlMg filter was used. The movie frame field of view was 256×380 pixels, corresponding to 20.9×31.0 arc min in the usual half-resolution, i.e., 2×2 pixels, images. The quarter-resolution (4×4 pixels) images were resized and combined with the half-resolution images in the movies. To track the TCH in time, the initial solar pointing of the movie frame was selectable and the center of the image frame was translated westward throughout the movie at a rate that compensates for solar rotation at the frame center. Image selection was set for one image per hour closest to even one-hour intervals throughout the day, with typically 15 to 23 images per day resulting for each TCH of Table 1. We viewed the data with logarithmic compression to enhance the faint features characteristic of the TCH boundaries. Each movie was viewed by stepping through the images as desired. The TCH locations were compared with full-disk daily magnetograms from Kitt Peak

National Observatory (KPNO) to determine the magnetic conditions in and around the TCHs.

2.2. General properties of transient coronal holes

The fourth column of Table 1 gives the number of TCHs observed in each event. In some cases we cannot exclude the possibility that one of two TCHs was obscured by overlying features, but in several cases the lone TCH was observed sufficiently close to disk center to exclude the presence of an obvious second TCH. The nine cases in which only one TCH was observed suggest that if TCHs must appear in pairs, the second can be much smaller than the first.

The fifth column of Table 1 gives estimated lifetimes of the TCHs derived by subtracting the times of first SXT observation of the TCH from the times of first SXT observation judged no longer showing the TCH. These values range from about 5 to 66 hrs and, because of the variable sizes of the SXT data intervals used for the study, the range should be considered only as indicative for some TCH lifetimes. Foreshortening and obscuration by foreground corona as the region approaches the limb biases the range towards shorter times. We have also estimated the characteristic widths of the TCHs near their times of observed maximum areas. These range from 4° to 20° with an average of 10°.

A striking characteristic of TCHs is that their boundaries change continuously. We find that the TCH inner boundaries (the ones closer to the arcades) generally move away from their associated arcades as the arcades expand in size perpendicular to the magnetic neutral lines. Figure 1 shows two good examples of TCHs with boundaries receding from the arcades. As shown in the sixth column of the table, this characteristic was evident in at least 17 of the 19 TCH events. An unexpected characteristic of the TCH outer boundaries is that they usually retreated away from the arcades for significant parts of their lifetimes. This was the case in at least 13 of the TCHs, as shown in the seventh column of the table. The outer boundaries were generally smooth and bright, rather than consisting of an array of footpoints of adjacent closed loops. This result can also be seen in the two events shown in Figure 1.

In no case did we see the interior TCH brightness increase systematically with time. Rather, the boundaries continued to contract until the TCH was no longer an identifiable feature. The expansion of the posteruptive arcade was usually responsible for a significant part of the area decrease, but we found no case in which the entire TCH area was eventually covered by the arcade. There was always appreciable contraction of the area, at least late in the TCH lifetime, from the outer boundary. In some cases there was not a completely closed boundary. The eighth column of the table shows that 5 TCHs were formed along existing CHs, and in those cases the TCH boundaries decreased until the TCHs merged with the long-lived CHs.

2.3. Magnetic-field characteristics of TCHs

The last column of the table gives a simple descriptor for the basic magnetic field configuration around the TCH, based on examinations of daily KPNO magnetograms. In all but four cases we found that the TCHs appeared to form near a region characterized by either a bend in the large-scale magnetic neutral line (NL) or the presence of a nearby active region. In the case of a bend in the NL, the TCH usually occupied a region of enhanced magnetic flux which resulted in the NL bend toward the TCH region, with the TCH region near the center of curvature of a convex NL. The first two TCHs of Figure 2 show examples of associated NL bends. In the cases of nearby active regions, the TCH fields were often weaker than those of surrounding regions, and the active-region fields facing the TCH areas were of the same polarities as the TCH fields. The third TCH of Figure 2 shows such an example.

3. Discussion

3.1. A basic concept for TCHs

The comparison of the TCH locations with the associated magnetic field maps and the coronal X-ray structures, as discussed in Section 2.3, suggests general features of the two configurations that lead to a TCH. The role of active-region fields in producing TCHs is not obvious to us, but we offer an explanation for the curved NL configuration in Figure 3. At the end of the arcade structure a NL curves around the site of the TCH. The connections from the TCH area are spread over a large region of the weaker fields on the opposite side, with those from part A aligned predominantly along the presumably highly stressed nonpotential fields of the site of the main eruptive X-ray event. The fields of part A are opened with the initial eruption and are the first to be reconnected into the posteruptive X-ray arcade. The larger loops from region B

are further removed from the main eruption and only erupt later to increase the TCH area, at the same time as the open fields of region A are reconnecting with a resulting decrease of the area of the TCH. The opening of the field lines proceeds smoothly and gradually through A and B.

There are several implications of this scenario. First, the TCHs are not required to occur in pairs, since the magnetic configuration at one end of an eruptive event may be different from that at the other end. We might expect only one TCH in an event, or possibly two. Because of the small number of TCHs easily seen in the 9-year SXT data set, the most likely number of TCHs in an event may be zero. Figure 3 contrasts with Figure 9 of Sterling et al. (2000), in which a highly sheared sigmoidal field line runs underneath a less-sheared magnetic field region to connect the positive polarity side of one end of the region to the negative polarity side of the other end. Those opposite polarity connected regions participate in the eruption to become TCHs. Another alternative is that of Figure 5 of Manoharan et al. (1996) in which the TCH regions are connected by a high magnetic loop which is activated by the underlying eruptive event. While we favor the schematic of our Figure 3, we can not rule out the other configurations as plausible explanations for some events.

Another implication of the TCH observations is that solar eruptive events can continue to develop over extended time scales of hours, consistent with the common occurrence of continued flow of material after a CME observed by the Helios photometers (Jackson and Webb, 1994) and by the LASCO coronagraph (Howard et al., 1997). Some evidence for this was presented by Kahler et al. (1998) for the large southern X-ray arcade event of April 14, 1994. The posteruptive X-ray arcade in that event continued to develop westward for at least 10 hours, but there was no dimming signature for that event to rule out the unlikely alternative possibility of a single relatively short-duration eruption. However, in most of the TCHs of this study we see simultaneous closing and opening of different magnetic field regions indicated by the motion of the TCH boundaries. This then implies that like active-region flares, CMEs may continue to undergo considerable evolution while still in their eruptive phases.

The TCHs appear to differ from their long-lived counterparts only in size and time scales. The formation and expansion of a TCH must occur by the opening of closed field lines, not by some interaction between open and closed field lines. Similarly, the TCH boundaries contract at least partly through magnetic reconnection of their open field lines with field lines of opposite polarity to close down and form the familiar posteruptive arcades. We suggest that the reconnection may also occur at the outer boundaries of TCHs without arcade formation.

3.2. Implications for the standard flare model

The standard model for LDE flares involves large-scale magnetic reconnection following an eruption. In the Yohkoh era this model, in its various forms, has come to be termed the CSHKP model (see for example Hudson and Cliver, 2001, for references, cartoons, and explanations). Our new view of TCH development, as described above, suggests that the opening and closing of large-scale magnetic fields may not be so simple as this model considers. For example, the arcade formation may not invariably close all of the newly opened field lines in long-lived TCHs. In addition, the lack of enhanced brightening during the TCH closing at the outer boundary suggests that if reconnection occurs there, it does not cause appreciable heating. Although not envisioned in the CSHKP model, we also see no evidence of localized patches of brightening within a TCH. This would be interpreted as energy release at the footpoint of an interplanetary magnetic cloud, resulting from 3D field-line reconnection as envisioned by Larson et al. (1997).

The continued gradual opening of the outer boundary of a TCH, even as the arcade expands into its inner boundary, poses a geometrical problem. This would not be possible in the 2D models and is difficult to envision in 3D (flux rope) models with small twist, because the interior parts of the ejection necessarily must force the outer parts of the corona open first. Similarly, the gradual closing of the TCH from the *outer* boundary flies in the face of the conventional wisdom regarding the gradual *upwards* motion of the reconnection point.

3.3. Where does the outer boundary reconnect?

The area of a TCH can only change via the opening or closing of magnetic field lines, and we have identified a clear pattern for a part of the re-closing to be unrelated to the flare arcade (region B in the schematic cartoon, Figure 3). Where do these field lines reconnect? The cartoon suggests that the larger-scale outer field lines of the erupting structure in fact do not re-close in the arcade, or even in the vicinity of the neutral line. In order to close, the newly opened field lines must therefore find an independent source of open field lines of the opposite polarity. We speculate that such field lines could be found in previously existing coronal holes, in open-field inclusions in the quiet corona, or in sunspot umbrae. Any one of these possibilities greatly complicates the straightforward picture assumed in the standard model.

3.4. Consequences for the fluxrope footpoint model

In Section 1 we discussed the associations between TCHs and interplanetary magnetic flux ropes made by various authors. Those associations have been made without regard to the temporal development of the TCHs or to the possible impact of that development on the flux rope observations at 1 AU. Two of the TCHs in our Table have been associated with flux ropes, so we can examine those events in some detail.

The TCH of October 14, 1995 has been associated with an interplanetary shock and a magnetic cloud observed at 1 AU on October 18, 1995 (Smith et al., 1997; Larson et al., 1997). That TCH lay in a negative polarity region between the reverse polarity AR 7912 and normal polarity AR 7910, as shown at the top of Figure 4. Formation of the TCH occurred close to the maximum of a C1 X-ray flare in AR 7912. On October 18-20, 1995, a magnetic cloud was observed by the WIND spacecraft at 1 AU. It was interpreted by Larson et al. (1997) as a negative polarity flux rope with connection to the negative polarity region of AR 7912, from which flare energetic electrons were injected and then observed at WIND. The area of the TCH contracted from about 12:00 UT on October 14 until it disappeared about 10:00 UT on October 15.

The TCH of May 12, 1997 has been associated with a halo CME, an interplanetary shock and magnetic cloud, and a geomagnetic storm (Webb et al., 2000a). Observations with EIT showed a pair of dimmings in the 195Å line at 06:22 UT located northeast and southwest of AR 8038. Webb et al. (2000b) hypothesized that the double dimming regions were the feet of the rising coronal flux loops that became the magnetic cloud at 1 AU. From Hα, EIT, and LASCO coronagraph observations they found an event onset time of 04:50 UT. To estimate the magnetic flux of the flux loop at 1 AU, they calculated the total magnetic flux in photospheric areas which showed dimming in the EIT images. Although they state that the dimmings were first fully formed in the 05:24 UT image, they used the brightness difference image formed from the earlier 05:07 and 04:50 UT EIT images to determine the mask for the photospheric magnetic field areas. Those areas in their Figure 3 are much smaller than the dimming regions shown in the 06:22 UT EIT image of their Figure 1, so the relationship between the dimming regions of the direct images and those used for the magnetic flux measurements is in question. Furthermore, their southern region of flux eruption included part of the leader sunspot, a result possibly due to projection effects of the N20 location of the erupting region. Although the TCHs are not well defined in the SXT images, the boundaries seen in the 06:52 UT AlMg image match well the outline of the 06:22 UT EIT image. That is approximately the time when Thompson et al. (1998) report the maximum decrease of emission measure in the dimming regions. The Al.1 images of the bottom of Figure 4 show that the better observed northern TCH continued to contract as the X-ray arcade expanded into the TCH northern and western regions. That TCH was no longer visible by 15:41 UT, as shown in Figure 4.

The association of the TCHs with the magnetic clouds in these two cases is in agreement with the observed cloud polarities, and in the case of the May 12, 1997 TCH, with the calculated cloud magnetic flux and axial direction. However, we have seen that there is reason to question the magnetic flux calculation of the May 12 TCH event. In both these TCHs the magnetic fields are weak, as can be seen from Figure 4, so the resulting eruptive TCH magnetic fluxes may be too small to match the magnetic cloud flux. Furthermore, for the May 12 event the claimed source region of the cloud is confined to the active region, as Figures 3 and 5 of Webb et al. (2000b) make clear. This stands in contrast to the much larger EIT dimming source regions found for energetic CMEs by Thompson et al. (2000). We therefore believe that the identification of TCHs as the source regions of magnetic clouds is unjustified. Even if this association is correct in some cases, the lifetimes of TCHs, less than 48 hours in nearly all cases, is shorter than the 3-5 day ages of the magnetic clouds observed at 1 AU. This implies that a complete disconnection has occurred between the TCHs and the magnetic clouds, even though heat flux and energetic electron observations show at least partial magnetic connection of the magnetic clouds to the corona (Larson et al., 1997).

4. Conclusions

An examination of the development of 19 TCHs shows that their boundaries evolve in time, simultaneously losing area to the reconnection of open field lines close to the NL and gaining area as closed field lines more distant from the NL continue to open. This indicates that the process of field line opening in the associated CMEs may continue for hours after the initial eruption. TCHs disappear within typically 48 hr by contraction of the boundaries rather than by any internal brightening. TCHs appear to form in areas of high field intensity with resulting bends in magnetic NLs or in weak field regions near the same-polarity strong fields of adjacent active regions. Based on the shifting boundaries, short lifetimes, and generally weak fields of the TCHs, we question whether they can be associated with magnetic clouds.

The prevalence of single TCHs, or of strongly asymmetrical pairs of TCHs, is a striking feature of our data set. We conjecture that the matching footpoints must occur in such places as sunspot umbrae, diffuse structures embedded in the general corona, or remote new coronal holes obscured by foreground corona.

Acknowledgments. A Window on Asia grant from the Air Force Office of Scientific Research supported the work of S. K. We thank T. Kosugi for his hospitality during the stay of S. K. at the Institute of Space and Aeronautical Science. Hudson's work was supported under NASA contract NAS 8–37334. N. V. Nitta provided valuable assistance with Yohkoh software. NSO/Kitt Peak National Observatory data used here are produced cooperatively by NSF/NOAO, NASA/GSFC, and NOAA/SEL.

References

Howard, R. A., et al., Observations of CMEs from SOHO/LASCO, in Coronal Mass Ejections, (eds. N. Crooker, J. A. Joselyn, and J. Feynman) AGU Geophysical Monograph 99, 17, 1997.

Hudson, H. S., and E. W. Cliver, Observing coronal mass ejections without coronagraphs, JGR, in press, 2001.

Hudson, H. S., and D. F. Webb, Soft X-ray signatures of coronal ejections, in Coronal Mass Ejections, (eds. N. Crooker, J. A. Joselyn, and J. Feynman) AGU Geophysical Monograph 99, 27, 1997.

Hudson, H. S., J. R. Lemen, O. C. St. Cyr, A. C. Sterling, and D. F. Webb, X-ray coronal changes during halo CMEs, GRL, 25, 2481, 1998.

Jackson, B. V., and D. F. Webb, The masses of CMEs measured in the inner heliosphere, Proc. Third SOHO Workshop, ESA SP-373, 233, 1994.

Kahler, S. W, and D. Moses, Discrete changes in coronal hole boundaries, Astrophys. J., 362, 728, 1990.

Kahler, S. W., H. V. Cane, H. S. Hudson, V. G. Kurt, Y. V. Gotselyuk, R. J. MacDowall, and V. Bothmer, The solar energetic particle event of April 14, 1994, as a probe of shock formation and particle acceleration, JGR, 103, 12,060 (1998).

Khan, J. I., Y. Uchida, A. H. McAllister, Z. Mouradian, I. Soru-Escaut, and E. Hiei, A flare-associated filament eruption observed in soft X-rays by Yohkoh on 1992 May 7, Astron. Astrophys., 336, 753, 1998.

Larson, D. E., et al., Tracing the topology of the October 18-20, 1995, magnetic cloud with 0.1-10^2 keV electrons, GRL, 24, 1911, 1997.

Manoharan, P. K., L. van Driel-Gesztelyi, M. Pick, and P. Demoulin, Evidence for large-scale solar magnetic reconnection from radio and X-ray measurements, Astrophys. J., 468, L73, 1996.

Rust, D. M., Coronal disturbances and their terrestrial effects, Space Sci. Rev., 34, 21, 1983.

Shodhan, S., N. U. Crooker, S. W. Kahler, R. J. Fitzenreiter, D. E. Larson, S. F. Martin, S. P. Plunkett, and D. M. Rust, Counterstreaming electrons in magnetic clouds, J. Geophys. Res., 105, 27,261, 2000.

Smith, Z., S. Watari, M. Dryer, P. K. Manoharan, and P. S. McIntosh, Identification of the solar source for the 18 October 1995 magnetic cloud, Solar Phys., 171, 177, 1997.

Sterling, A. C., and H. S. Hudson, Yohkoh SXT observations of X-ray "dimming" associated with a halo coronal mass ejection, Astrophys. J., 491, L55, 1997.

Sterling, A. C., H. S. Hudson, B. J. Thompson, and D. M. Zarro, Yohkoh SXT and SOHO EIT observations of sigmoid-to-arcade evolution of structures associated with halo coronal mass ejections, Astrophys. J., 532, 628, 2000.

Thompson, B. J., S. P. Plunkett, J. B. Gurman, J. S. Newmark, O. C. St. Cyr, and D. J. Michels, SOHO/EIT observations of an Earth-directed coronal mass ejection on May 12, 1997, GRL, 25, 2465, 1998.

Thompson, B. J., E. W. Cliver, N. Nitta, C. Delannée, and J.-P. Delaboudiniére, Coronal dimmings and energetic CMEs in April-May 1998, GRL, 27, 1431, 2000.

Tsuneta, S., L. Acton, M. Bruner, J. Lemen, W. Brown, R. Caravalho, R. Catura, S. Freeland, B. Jurcevich, M. Morrison, Y. Ogawara, T. Hirayama, T., and J. Owens, The soft X-ray telescope for the SOLAR-A mission, Sol. Phys., 136, 37, 1991.

Wang, Y.-M., and N. R. Sheeley, Jr., Understanding the rotation of coronal holes, Astrophys.

J., 414, 916, 1993.

Wang, Y.-M., S. H. Hawley, and N. R. Sheeley, Jr., The magnetic nature of coronal holes, Science, 271, 464, 1996.

Watanabe, T., et al., Coronal/interplanetary disturbances associated with disappearing solar filaments, Publ. Astron. Soc. Japan, 44, L199, 1992.

Watari, S., Y. Kozuka, M. Ohyama, and T. Watanabe, Soft X-ray coronal holes observed by the Yohkoh SXT, J. Geomag. Geoelectr., 47, 1063, 1995.

Webb, D. F., E. W. Cliver, N. U. Crooker, O. C. St. Cyr, and B. J. Thompson, Relationship of halo coronal mass ejections, magnetic clouds, and magnetic storms, J. Geophys. Res., 105, 7491, 2000a.

Webb, D.F., R. P. Lepping, L. F. Burlaga, C. E. DeForest, D. E. Larson, S. F. Martin, S. P. Plunkett, and D. M. Rust, The origin and development of the May 1997 magnetic cloud, J. Geophys. Res., 105, 27251, 2000b.

S. W. Kahler, Air Force Research Laboratory

H. S. Hudson, Solar Physics Research Corporation

Received April 30, 2001

To appear in the *Journal of Geophysical Research*, 2001.

Table 1. Table of Transient Coronal Holes

Date and time, UT				Location	N[a]	T[b]	Arc[c]	Loop[d]	Comp/Part[e]	B Field[f]
28	Sep	1991	13:50	N15W05	1	>3	??	Y	P, along CH	Y, NL bend
11	Mar	1992	02:16	S30E10	1	>31	Y	Y	C	Y, NL bend
07	Jun	1992	06:25	N20W15	2	26	Y	Y	C	Y, AR
05	Nov	1992	00:10	N05W05	2	66	Y	Y	P, along CH	Y, NL bend
16	Jan	1993	12:20	S40W25	2	8	Y	Y	C	Y, NL bend
25	Oct	1994	11:44	N15W25	2	>19	Y	??	C	Y, NL bend
12	May	1995	17:39	S15E25	2	5	Y	Y	P, along CH	Y, NL bend; AR
14	Oct	1995	08:34	S10E10	1	26	Y	??	??	Y, AR
07	Apr	1997	16:02	S40E40	1	<21	Y	??	C	Y, NL bend
12	May	1997	06:52	N35W05	2	9	Y	N	C	??
23	Oct	1997	13:45	N20E10	2	5	Y	Y	N	Y, NL bend; AR
21	Jan	1998	08:13	S55W15	1	<24	Y	N	P, along CH	N
22	Jun	1998	06:13	S40E05	1	11	Y	N	C	Y, AR
15	Oct	1998	01:15	N20E25	2	16	Y	Y	C	Y, NL bend
12	Sep	1999	00:41	N05W55	2	>40	Y	Y	C	??
12	Sep	1999	05:06	N25W15	1	9	Y	Y	C	N
29	Apr	2000	13:09	N10E05	1	6	Y	Y	P, along CH	Y, AR

Table 1. (continued)

Date and time, UT				Location	N[a]	T[b]	Arc[c]	Loop[d]	Comp/Part[e]	B Field[f]
11	Jun	2000	13:09	N00E10	1	43	??	Y	??	Y, AR
15	Jul	2000	03:12	S20W10	2	36	Y	Y	C	Y, AR

[a]Number of coronal holes

[b]Duration, hr

[c]Here "Y" means that the arcade diminished the TCH area.

[d]Here "Y" means that the loops at the far boundary receded.

[e]Complete or partial boundary

[f]Could a distinct magnetic configuration be recognized? AR = "active region"; NL = "neutral line"

Figure 1. Top: Al filter SXT images showing a pair of transient coronal holes (TCHs) forming near a bend in the magnetic neutral line (NL) as an arcade developed along a northeast-southwest NL on November 5, 1992. The large positive polarity TCH developed adjacent to a small midlatitude coronal hole, and a small negative polarity TCH, shown by the arrow in the 19:26 UT image, developed to the east. The arcade boundaries, one of which is shown by the black arrow in the 09:22 UT image, advanced into the areas of the TCHs throughout the event. Initially the outer boundary of the western TCH receded (04:11 UT), but then also contracted (09:22, 19:26 UT). The contour lines show the TCH boundaries at the times of the first and last images, interchanged, for reference. The last image is the KPNO magnetogram with positive and negative polarities shown as white and black, respectively. Bottom: AlMg filter SXT images showing a large TCH forming in a negative polarity field region south of a bend in the NL on October 15, 1998. The arcade boundary shown by the black arrow on the 08:09 UT image expanded into the TCH from the north as the loop system lying parallel to the southern boundary receded away from the NL. Loop brightening in the south and arcade expansion in the north then forced the TCH boundaries to contract to a small area at 13:19 UT. The last image is the KPNO magnetogram with positive and negative polarities shown as white and black, respectively.

Figure 2. Three comparisons between TCHs and aligned KPNO magnetograms. Lines on the latter indicate approximate TCH boundaries. Left: March 11, 1992. The TCH lies in an area of strong positive fields north of an extended east-west NL where the arcade forms. Middle: October 25, 1994. The northern TCH lies in a negative polarity region along a bend of the NL to the northwest from AR 7792. The southern TCH is characterized by somewhat stronger fields than those across the north-south NL. Right: June 22, 1998. The TCH lies in a positive polarity region adjacent to the trailing positive polarity fields of AR 9049.

Figure 3. Cartoon showing a suggested configuration leading to the formation of a transient coronal hole (TCH). The dashed line is a magnetic neutral line (NL) with a curve, or bend. Top: The magnetic field lines of the TCH are connected to a larger area of weaker fields on the opposite side of the NL. As the strongly sheared fields erupt along the NL, those TCH fields from region A extending into the sheared region also erupt. Bottom: As the posteruptive arcade forms, the first TCH fields to open are closed in the reconnection process. At the same time, the fields of the farther region B of the TCH proceed to open and increase the TCH area.

Figure 4. Top row: AlMg SXT images and KPNO magnetogram. The TCH of October 14, 1995, lies in a weak negative polarity region surrounded by the negative polarity fields of AR 7912 in the east and AR 7910 in the west (the diagonal line in the second panel shows the location). AR 7913 lies south of the TCH. The initiation of the TCH follows a flare in AR 7912. The developing arcade along the NL northwest of AR 7912 and loops from AR 7913 expand into the TCH, causing the TCH area to vanish on October 15. Bottom row: Al.1 SXT images and KPNO magnetogram. The two TCHs of May 12, 1997, indicated by the lines, lie in a weak negative polarity region in the north and a weak positive polarity region in the south. The arcade extends to the north of the northern TCH along a bend of the NL to the northeast. The more easily observed northern TCH has vanished by 23:05 UT.

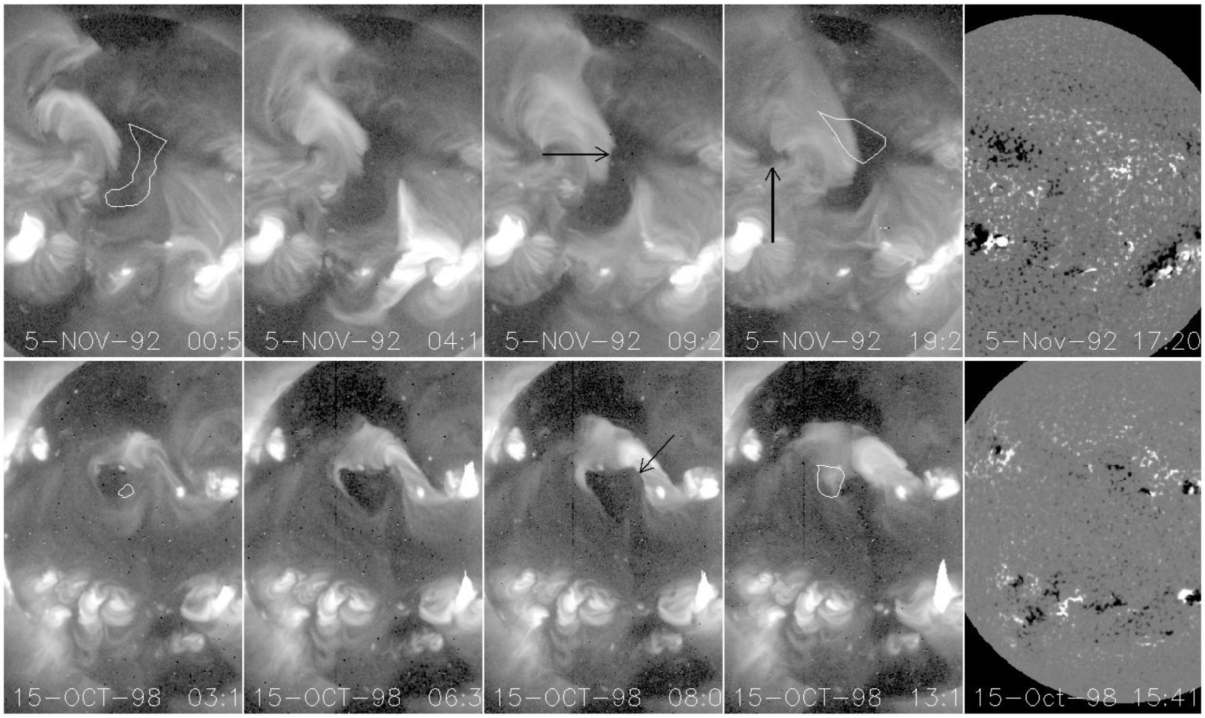

5-NOV-92 00:5
5-NOV-92 04:1
5-NOV-92 09:2
5-NOV-92 19:2
5-Nov-92 17:20
15-OCT-98 03:1
15-OCT-98 06:3
15-OCT-98 08:0
15-OCT-98 13:1
15-Oct-98 15:41

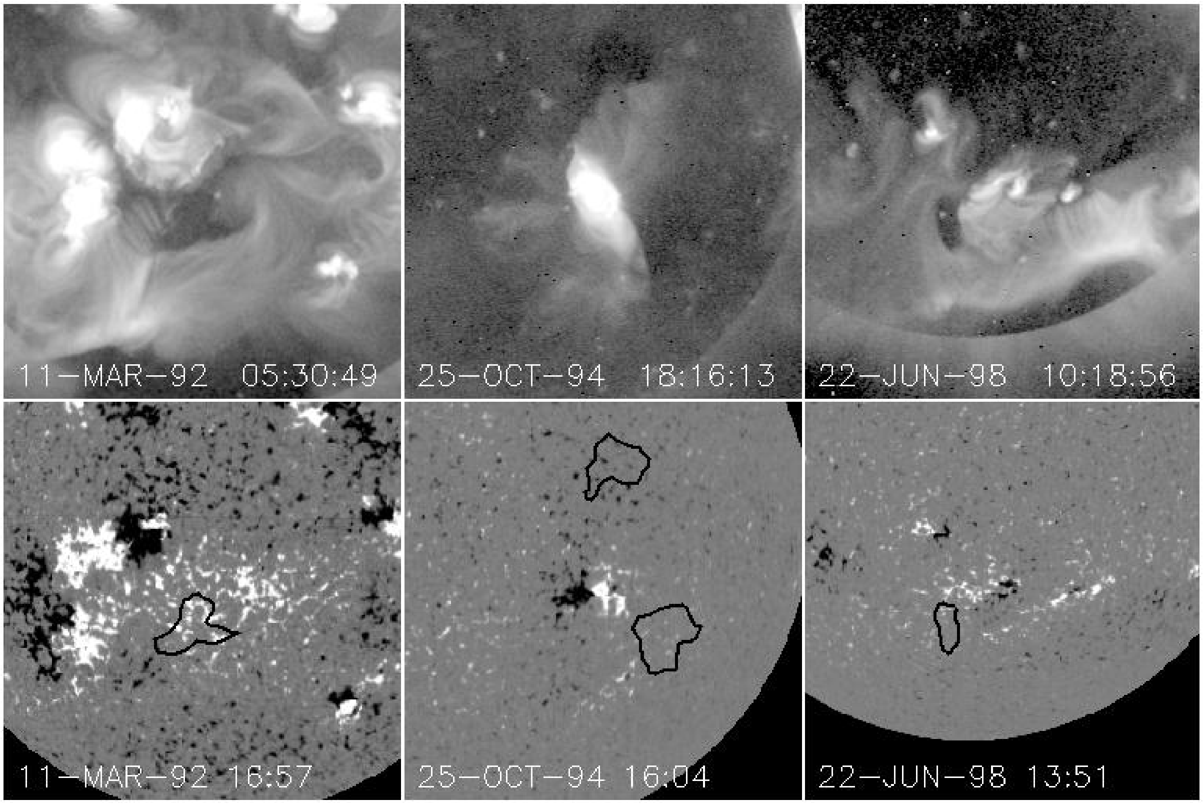
11−MAR−92 05:30:49
25−OCT−94 18:16:13
22−JUN−98 10:18:56
11−MAR−92 16:57
25−OCT−94 16:04
22−JUN−98 13:51

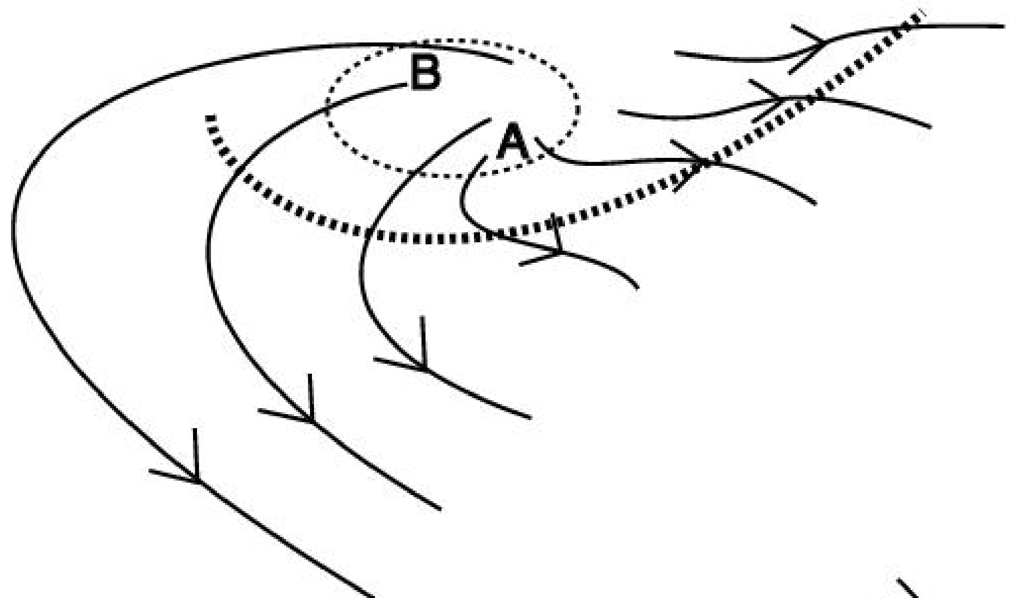
B
A

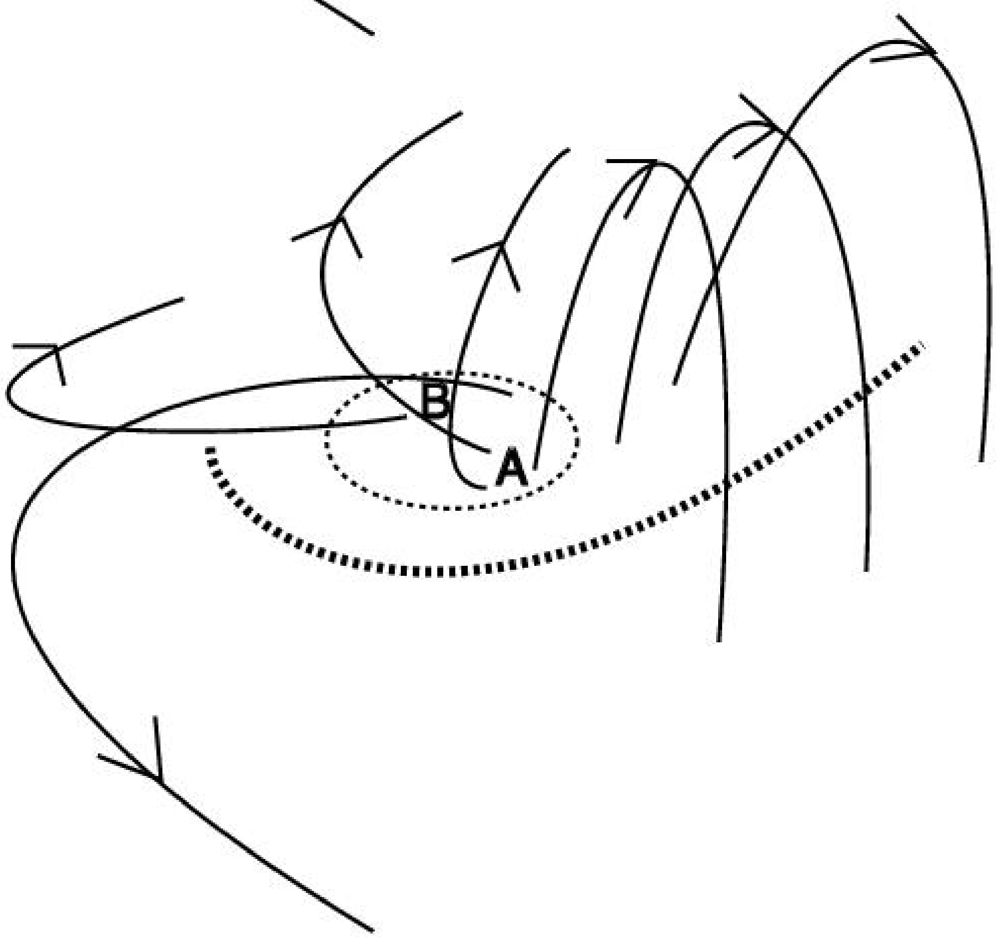
B
A

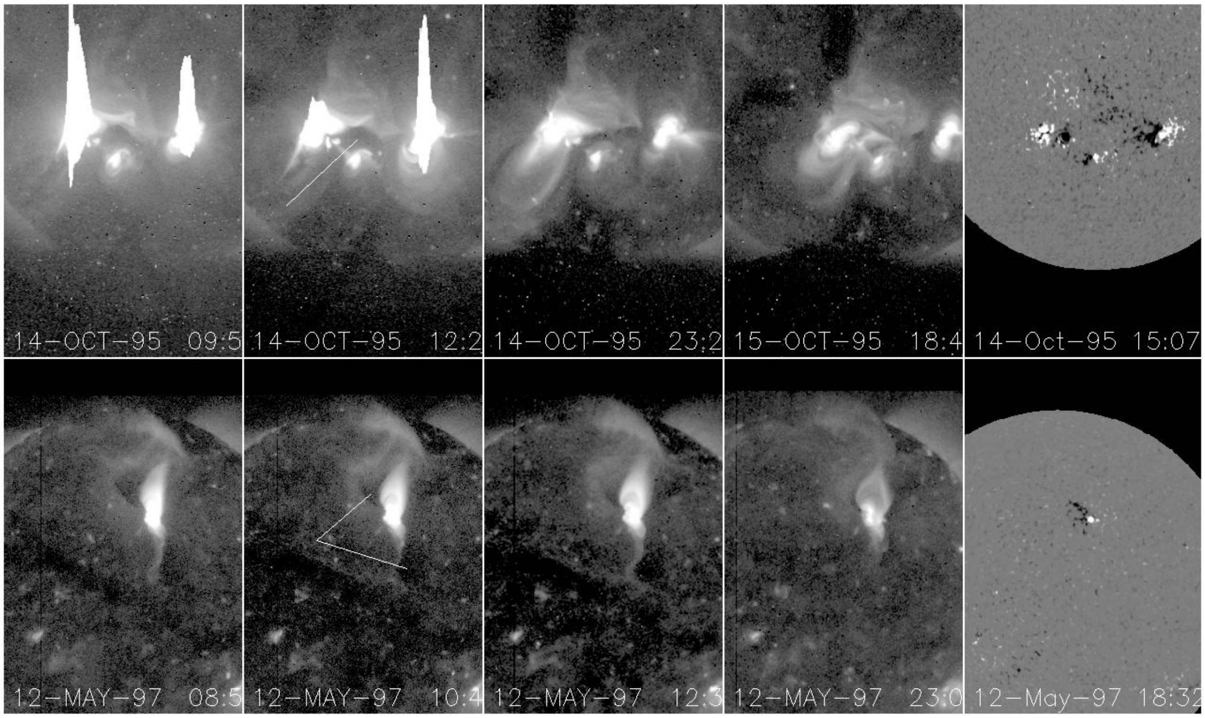
14-OCT-95 09:5
14-OCT-95 12:2
14-OCT-95 23:2
15-OCT-95 18:4
14-Oct-95 15:07
12-MAY-97 08:5
12-MAY-97 10:4
12-MAY-97 12:3
12-MAY-97 23:0
12-May-97 18:32